7-1-2006

Transport of galectin-3 between the nucleus and cytoplasm. I. Conditions and signals for nuclear import

Peter J. Davidson
Michigan State University

Su Yin Li
Michigan State University

Andrew G. Lohse
Calvin University

Rianna Vandergaast
Calvin University

Glycobiology vol. 16 no. 7 pp. 602–611, 2006
doi:10.1093/glycob/cwj088
Advance Access publication on February 9, 2006

Transport of galectin-3 between the nucleus and cytoplasm. I. Conditions and signals for nuclear import

Peter J. Davidson[2], Su-Yin Li[3], Andrew G. Lohse[5], Rianna Vandergaast[5], Elisa Verde[5], Andrea Pearson[5], Ronald J. Patterson[4], John L. Wang[3], and Eric J. Arnoys[1,3]

[2]Cell and Molecular Biology Program, [3]Department of Biochemistry, and [4]Department of Microbiology, Michigan State University, East Lansing, MI 48824; and [5]Department of Chemistry and Biochemistry, Calvin College, Grand Rapids, MI 49546

Received on December 7, 2005; revised on January 25, 2006; accepted on February 3, 2006

Galectin-3, a factor involved in the splicing of pre-mRNA, shuttles between the nucleus and the cytoplasm. We have engineered a vector that expresses the fusion protein containing the following: (a) green fluorescent protein as a reporter of localization, (b) bacterial maltose-binding protein to increase the size of the reporter polypeptide, and (c) galectin-3, whose sequence we wished to dissect in search of amino acid residues vital for nuclear localization. In mouse 3T3 fibroblasts transfected with this expression construct, the full-length galectin-3 (residues 1–263) fusion protein was localized predominantly in the nucleus. Mutants of this construct, containing truncations of the galectin-3 polypeptide from the amino terminus, retained nuclear localization through residue 128; thus, the amino-terminal half was dispensable for nuclear import. Mutants of the same construct, containing truncations from the carboxyl terminus, showed loss of nuclear localization. This effect was observed beginning with truncation at residue 259, and the full effect was seen with truncation at residue 253. Site-directed mutagenesis of the sequence ITLT (residues 253–256) suggested that nuclear import was dependent on the IXLT type of nuclear localization sequence, first discovered in the *Drosophila* protein Dsh (dishevelled). In the galectin-3 polypeptide, the activity of this nuclear localization sequence is modulated by a neighboring leucine-rich nuclear export signal.

Key words: galectins/nuclear export/nuclear import/nucleocytoplasmic transport/splicing factor

Introduction

Galectin-3 (Gal3) is a member of a family of galactose-specific carbohydrate-binding proteins found in a variety of cell types (Barondes *et al*., 1994). It is predominantly an intracellular protein, being found in both the cytoplasm and the nucleus of cells (Liu *et al*., 2002). The nuclear localization of Gal3 was sensitive to ribonuclease treatment of permeabilized cells, prior to their fixation for analysis by immunofluorescence and immunoelectron microscopy (Laing and Wang, 1988; Hubert *et al*., 1995). Moreover, sedimentation of nucleoplasm over cesium sulfate density gradients identified Gal3 in fractions with densities corresponding to those reported for heterogeneous nuclear ribonucleoprotein complex (hnRNP) and small nuclear RNPs (snRNP). Because these RNPs play important roles in the nuclear processing of pre-mRNA, the possibility was raised that Gal3 was a splicing factor as well.

Indeed, using a cell-free assay, depletion and reconstitution experiments showed that Gal3 and another member of the galectin family, galectin-1 (Gal1), were redundant but required factors in the splicing of pre-mRNA (Dagher *et al*., 1995; Vyakarnam *et al*., 1997). More recently, it was documented (Park *et al*., 2001) that Gal3 as well as Gal1 interacts with Gemin4, which has been characterized as one component of a macromolecular complex, designated as the SMN complex (Meister *et al*., 2002). The functional significance of this interaction appears to be in the early steps of spliceosome assembly. The addition of the NH_2-terminal domain of Gal3 or the COOH-terminal 50 amino acids of Gemin4 to splicing competent nuclear extracts inhibited splicing and blocked the conversion of early (H/E) complexes to active spliceosomes (Park *et al*., 2001).

The SMN complex is found both in the nucleus and in the cytoplasm. In the cytoplasm, the SMN complex is involved in the assembly of snRNPs (Fischer *et al*., 1997), prior to their entry into the nucleus to function as required components in the splicing of pre-mRNA. In the nucleus, the SMN complex is localized in discrete bodies called Gems (Liu and Dreyfuss, 1996) and appears to play a role in the "rejuvenation or recycling" of the snRNPs for supplying them to the intermediates (H/E complex) in spliceosome assembly (Pellizzoni *et al*., 1998). The association of Gal3 with the SMN complex raises the possibility that the protein also performs functions in both the nucleus and the cytoplasm and that it shuttles between the two compartments. Indeed, analysis of Gal3 localization in both nuclei of heterodikaryons (i.e., derived from fusion of a Gal3-expressing cell with a Gal3-null cell) provided definitive evidence for nucleocytoplasmic shuttling (Davidson *et al*., 2002).

Static observations on the nuclear versus cytoplasmic localization of Gal3 must reflect a balance between at least four key parameters: (a) nuclear import, (b) nuclear export, (c) cytoplasmic anchorage, and (d) binding and retention in the nucleus. As a first step in understanding how these parameters determine the nuclear versus cytoplasmic distribution of the protein, we wished to delineate the amino acid

[1]To whom correspondence should be addressed; e-mail: earnoys@calvin.edu

residues important for nuclear import. Two laboratories have attempted to define the region of the Gal3 polypeptide important for nuclear localization, with quite incongruent results. Gong *et al*. (1999) reported that the 11 residues at the amino terminus of Gal3 are involved in its translocation to the nucleus. On the other hand, Gaudin *et al*. (2000) showed that nuclear localization does not require the first 103 amino acid residues; rather, the carbohydrate-recognition domain (CRD) was sufficient for nuclear localization. The data derived from our present analysis support the conclusion of Gaudin *et al*. (2000) and indicate that specific residues near the carboxyl terminus are required for nuclear import. In addition, we also provide some insights into explaining certain observations that appeared to have confounded the latter group.

Results

A GFP reporter construct for the localization of Gal3

To define the residues critical for nuclear import and nuclear export of Gal3, we developed a reporter construct expressing a fusion protein containing Gal3 (~33 kDa) and green fluorescent protein (GFP) (~27 kDa). This fusion protein also contains bacterial maltose-binding protein (MBP) (~40 kDa) to serve as a "spacer" that increases the molecular weight of the reporter polypeptide. This was done to ensure that the size of the reporter polypeptide would exceed the exclusion limit of nuclear pores (40–60 kDa), even when the Gal3 polypeptide was decreased significantly through deletion mutagenesis.

The cDNA for Gal3 was digested with EcoRI and ligated into the corresponding restriction site in the prokaryotic expression vector pMAL-c_2x. The success of this step was indicated by the following: (a) the same MBP–Gal3 fusion protein (~74 kDa) could be detected in bacterial lysates by immunoblotting with either anti-MBP or anti-Gal3; (b) the MBP–Gal3 fusion protein could be isolated on lactose affinity columns. This plasmid then served as the template for PCR amplification of the coding region corresponding to MBP–Gal3, and the product was ligated into the eukaryotic expression vector pEGFP-c_1. The authenticity of each of the constructs was checked by DNA sequencing. This initial construct and its variants were used to transfect mouse 3T3 fibroblasts, and extracts of transfected cultures were subjected to western blotting with antibodies directed against the three parts of the expressed fusion protein: (a) anti-GFP, (b) anti-MBP, and (c) anti-Gal3. This was carried out to confirm that the predominant polypeptide bearing the GFP reporter group corresponded to the expected molecular weight of the fusion protein. Thus, the observed fluorescence signal can be ascribed to the localization of the construct under study.

Transfection of 3T3 cells with GFP resulted in the expression of a ~27 kDa polypeptide (Figure 1, lane 1) and fluorescence in both the nuclear and the cytoplasmic compartments (data not shown). This observation is consistent with the expectation that a ~30 kDa polypeptide would be able to diffuse across the nuclear pores, as well as with previous reports on the localization of GFP (Sherman *et al*., 2001; Alefantis *et al*., 2003). Western blotting of cells transfected

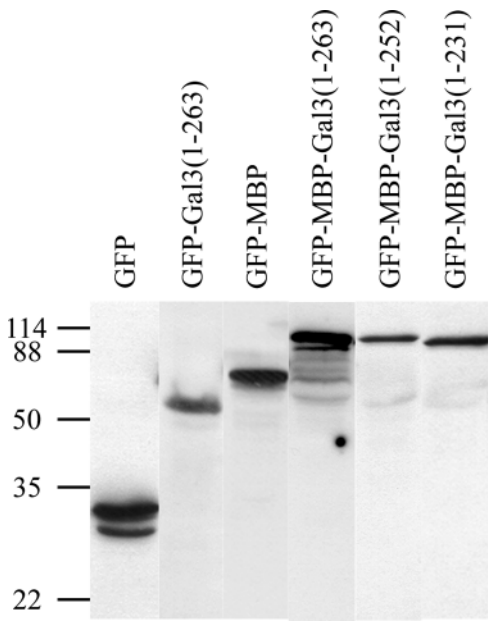

Fig. 1. Analysis of the fusion proteins expressed from the GFP reporter vector by western blotting. Lane 1, GFP; lane 2, GFP–Gal3(1–263); lane 3, GFP–MBP; lane 4, GFP–MBP–Gal3(1–263); lane 5, GFP–MBP–Gal3(1–252); lane 6, GFP–MBP–Gal3(1–231). Mouse 3T3 fibroblasts were transfected with the various constructs. Extracts (~50 μg total protein) derived from each of the transfected cultures were subjected to SDS–PAGE and immunoblotting with antibodies directed against GFP.

with GFP–MBP–Gal3(1–263) yielded a ~100 kDa polypeptide (Figure 1, lane 4), consistent with the sum of the molecular weights of the three parts of the fusion protein. Some GFP–MBP–Gal3(1–263) transfected cells exhibited fluorescence exclusively in the nucleus (N) (Figure 2, panel A), whereas other cells showed intensely nuclear fluorescence over a cytoplasmic background (N > C) (Figure 2, panel B).

Transfection with GFP-Gal3(1–263) yielded the expected ~60 kDa polypeptide (Figure 1, lane 2) and a fluorescence pattern similar to that for GFP–MBP–Gal3(1–263) (data not shown). Cells transfected with GFP-MBP yielded a ~67 kDa polypeptide (Figure 1, lane 3). GFP–MBP–Gal3(1–252) (Figure 1, lane 5) yielded the N < C (less nuclear labeling than cytoplasmic) fluorescence pattern (Figure 2, panel D) in >20% of the cells. The exclusively cytoplasmic (C) labeling pattern was found in the majority of cells transfected with GFP–MBP–Gal3(1–231) (Figure 2, panel E), which produced a ~96 kDa polypeptide (Figure 1, lane 6).

Comparison of the subcellular distribution of GFP–MBP–Gal3(1–263) and endogenous galectin-3

To ascertain whether the subcellular distribution of the GFP–MBP–Gal3(1–263) reporter construct reflected that of the endogenous protein, we compared the GFP fluorescence pattern against the localization of Gal3 in untransfected 3T3 fibroblasts as revealed by indirect immunofluorescence using a rat monoclonal antibody directed against the protein. Gal3 in 3T3 cells is found in both the nucleus and the cytoplasm simultaneously (Moutsatsos *et al*., 1987; Laing and Wang, 1988; Hubert *et al*., 1995; Davidson *et al*., 2002). In any given population of cells, one

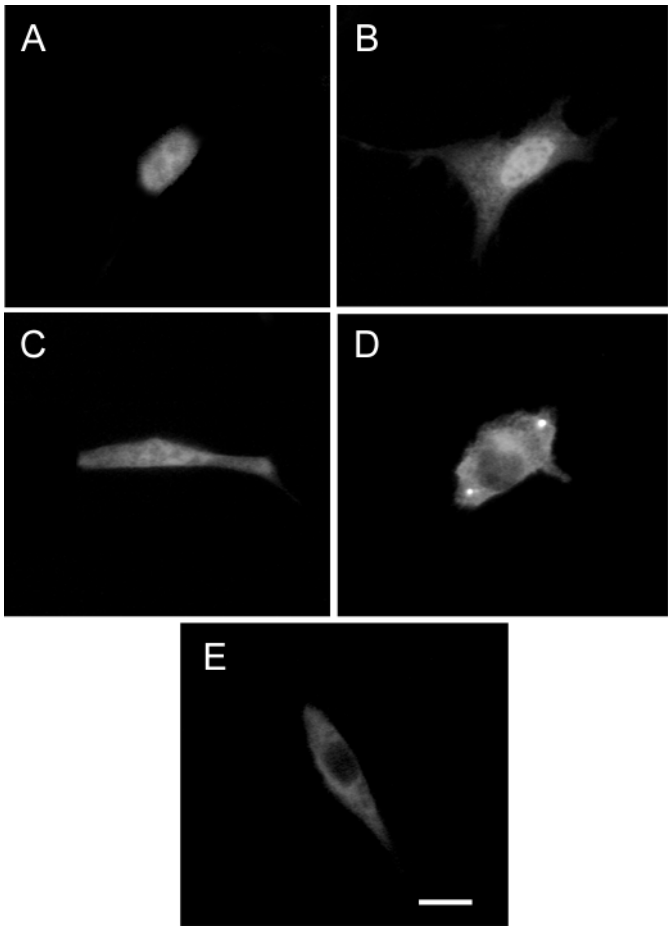

Fig. 2. Representative fluorescence micrographs illustrating the N, N > C, N~C, N < C, and C labeling patterns. (**A**) N, exclusively nuclear; (**B**) N > C, intensely nuclear over a cytoplasmic background; (**C**) N ~ C, equal distribution between the nucleus and cytoplasm; (**D**) N < C, less nuclear labeling than the cytoplasm; and (E) C, exclusively cytoplasmic. Bar = 10 μm.

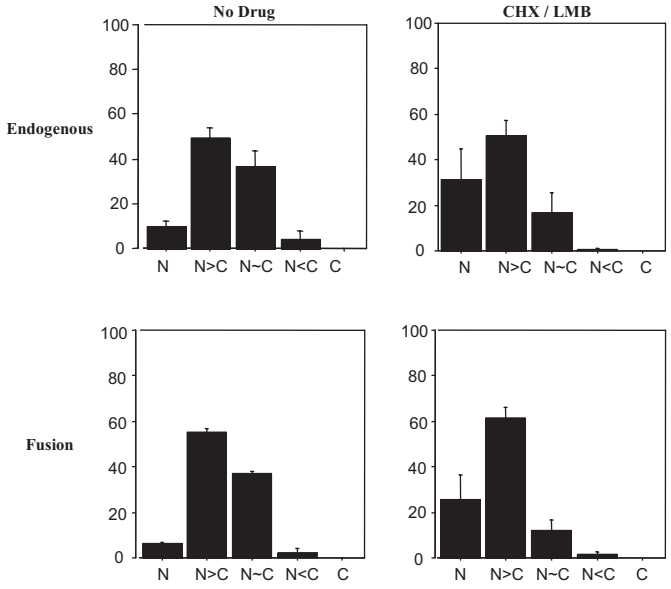

Fig. 3. Comparison of the histograms of fluorescence patterns obtained with GFP–MBP–Gal3(1–263) with endogenous Gal3 in 3T3 fibroblasts. The localization of GFP–MBP–Gal3(1–263) (Fusion) was monitored by GFP fluorescence; the localization of endogenous Gal3 in untransfected cells (Endogenous) was determined by indirect immunofluorescence using a rat monoclonal antibody against Gal3, the anti-Mac2 antibody. The fluorescence distributions were compared both in the presence and in the absence of a combination of the drugs, LMB (5.4 ng/ml) + CHX (10 μg/ml). The data represent the averages of triplicate determinations with standard error of the mean.

rarely finds exclusively nuclear or exclusively cytoplasmic fluorescence. Therefore, for this and all subsequent data, including those in the accompanying manuscript, comparisons are made on a quantitative basis by scoring the fluorescence in each cell in one of five categories: N, N > C, N ~ C, N < C, and C (as illustrated in Figure 2). The histograms of the fluorescence patterns for GFP–MBP–Gal3(1–263) and endogenous Gal3 were similar (Figure 3). This conclusion is supported by a chi-square analysis, which showed that the two distributions were not significantly different ($p = 0.048$).

In previous studies, we had documented that treatment of mouse and human fibroblasts with leptomycin B (LMB) resulted in the accumulation of Gal3 in the nucleus, as revealed by an accentuation of the nuclear staining pattern (Tsay *et al.*, 1999; Openo *et al.*, 2000). LMB inhibits the interaction between the CRM1 export receptor and a leucine-rich nuclear export signal (NES) on the cargo (Ossareh-Nazari *et al.*, 1997). In the present experiments, we included cycloheximide (CHX) (10 μg/ml) during the incubation with LMB (10 nM) to exclude complications that might be introduced by newly synthesized proteins (e.g., due to different rates of synthesis of the endogenous protein versus the fusion protein). Again, the histograms of the fluorescence patterns for GFP–MBP–Gal3(1–263) and endogenous Gal3 were very similar ($p = 0.033$) (Figure 3). More important, the data clearly showed that treatment with LMB shifted the fluorescence distribution "to the left," in favor of the nucleus. Chi-square analyses revealed significant differences between the following: (a) endogenous (no drug) versus endogenous (CHX/LMB) ($p < 0.0001$) and (b) fusion (no drug) versus fusion (CHX/LMB) ($p < 0.0001$).

Effects of truncation of the amino-terminal domain on localization

Using site-directed mutagenesis, EcoRI sites were inserted at various positions in the Gal3 polypeptide. Mutants, with truncation from the amino terminus of various lengths, were generated after restriction enzyme digestion and religation and were then analyzed as GFP–MBP–Gal3 fusion proteins. The histograms of fluorescence patterns for GFP–MBP–Gal3(74–263) and GFP–MBP–Gal3(121–263) (Figure 4) were essentially the same as those of the full-length protein, GFP–MBP–Gal3(1–263) (Fusion in Figure 3). Chi-square analyses revealed no significant differences between the following: (a) full-length versus 74–263 ($p = 0.6467$) and (b) full-length versus 121–263 ($p = 0.154$). This suggests that the amino-terminal half of the Gal3 polypeptide was dispensable for nuclear localization.

Beginning at residue 128, there was a shift of the histogram distribution "to the right," representing loss of nuclear localization in favor of the cytoplasm (Figure 4).

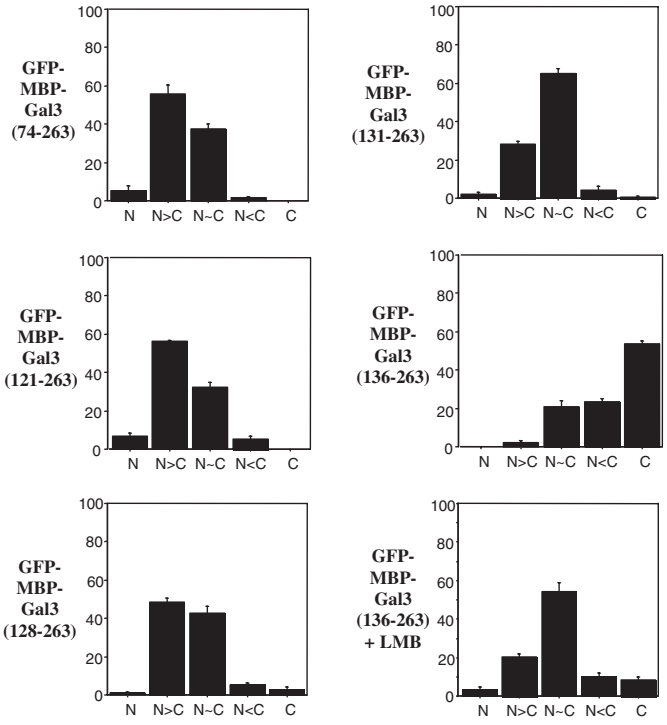

Fig. 4. Comparison of the histograms of fluorescence distributions for GFP–MBP–Gal3(1–263) mutants that are truncated from the amino terminus. The effect of LMB was tested at a concentration of 5.4 ng/ml. The data represent the averages of triplicate determinations with standard error of the mean.

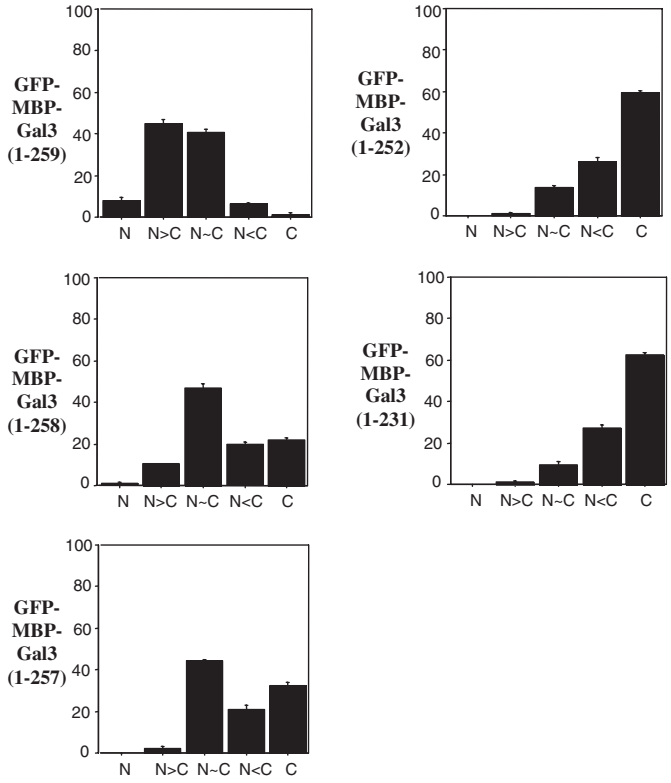

Fig. 5. Comparison of the histograms of fluorescence distribution for GFP–MBP–Gal3(1–263) mutants that are truncated from the carboxyl terminus. The data represent the averages of triplicate determinations with standard error of the mean.

This shift became quite prominent in GFP–MBP–Gal3(131–263) [chi-square of the histograms, GFP–MBP–Gal3(1–263) in Figure 3 versus GFP–MBP–Gal3(131–263) in Figure 4 ($p < 0.0001$)]. In GFP–MBP–Gal3(136–263), the predominant fluorescence pattern was cytoplasmic (Figure 4). Essentially identical results were obtained for GFP–MBP–Gal3(146–263) (data not shown) (chi-square of the latter two histograms, $p = 0.7284$).

Effects of truncation from the carboxyl terminus

Using site-directed mutagenesis to insert stop codons, we found that deletion of the last four amino acids of the Gal3 polypeptide did not significantly alter the localization. For example, the histogram of fluorescence patterns for GFP–MBP–Gal3(1–259) (Figure 5) was similar to that of the parent protein, GFP–MBP–Gal3(1–263) (Fusion in Figure 3) ($p = 0.0015$). Truncation of residue 259 [i.e., GFP–MBP–Gal3(1–258)], however, resulted in a shift of the histogram "to the right," reflecting more cells exhibiting cytoplasmic localization [Figure 5; chi-square analysis: GFP–MBP–Gal3(1–263) versus GFP–MBP–Gal3(1–258), $p < 0.0001$].

This shift became more pronounced in GFP–MBP–Gal3(1–257) (Figure 5) and reached its full effect upon truncation at residue 253 (GFP–MBP–Gal31–252). Its histogram was significantly different from both GFP–MBP–Gal3(1–263) ($p<0.0001$) and GFP–MBP–Gal3(1–257) ($p<0.0001$). When the truncation was made at residue 232 (GFP–MBP–Gal3(1–231) (~96 kDa, Figure 1, lane 5), there was no further shift in the histograms [GFP–MBP–Gal3(1–252) versus GFP–MBP–Gal3(1–231), $p = 0.398$]. More than 60 of the transfected cells had an exclusively cytoplasmic localization, as evident by examining either the micrograph (Figure 2, panel E) or the histogram (Figure 5). These results strongly suggest that the carboxyl-terminal portion of the Gal3 polypeptide, immediately upstream of residue 259, was important for nuclear localization.

Site-directed mutagenesis of residues 253–256

Site-directed mutagenesis was carried out on individual residues in the carboxyl-terminal region bounded by residues 252 and 257. Mutation at each residue appeared to affect nuclear localization of the GFP fusion reporter (Figure 6). Quite strikingly, however, the T254A mutation appeared to be the least deleterious to nuclear localization. This was of interest because the sequence IXLT was recently identified to be important for nuclear localization of the *Drosophila* protein Dsh (dishevelled) (Itoh *et al*., 2005). Residues 253–256 of the Gal3 sequence are ITLT, and thus the Thr at residue 254 corresponds to the variable X in the IXLT signal. The majority of the cells transfected with the double mutant GFP–MBP–Gal3(1–263; I253A; L255A) showed either N < C or exclusively C localization (data not shown). Moreover, the triple mutant, GFP–MBP–Gal3(1–263; I253A; L255A; T256A) showed cytoplasmic localization (Figure 6), as was found with *Drosophila* Dsh protein (Itoh *et al*., 2005).

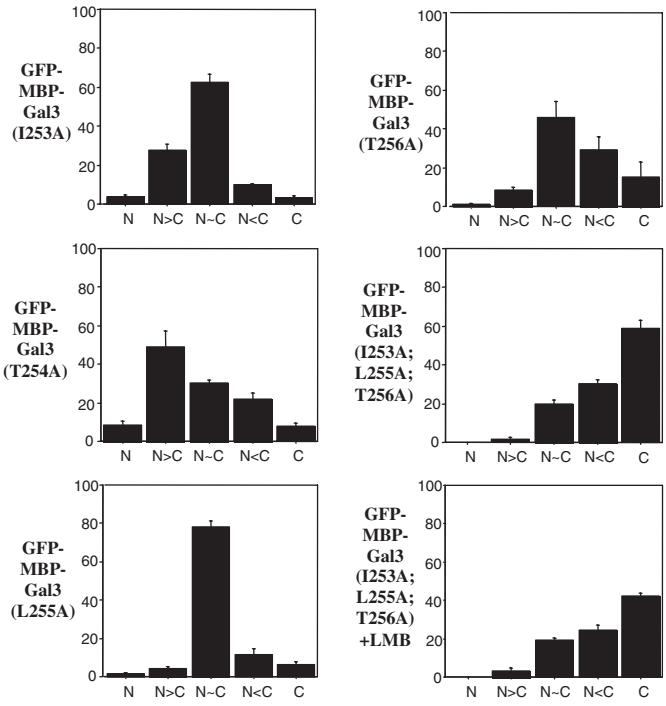

Fig. 6. Comparison of the histograms of fluorescence distribution for site-directed mutants of GFP–MBP–Gal3(1–263) at residues 253–256. The effect of LMB was tested at a concentration of 5.4 ng/ml. The data represent the averages of triplicate determinations with standard error of the mean.

Complications arising from an NES and insights provided by LMB

The identification of residues 253–256 as important for nuclear localization raises the question why GFP–MBP–Gal3(136–263) yielded cytoplasmic localization, despite the fact that it clearly contained these residues. Three key facts were considered to be important in rationalizing these results. First, X-ray crystallography of the Gal3 CRD (Seetharaman *et al.*, 1998) showed that the structure is composed of two β-pleated sheets associating in a sandwich-like arrangement, connected by an α-helix (Figure 7B). Second, in the accompanying manuscript (Li *et al.*, 2006), we document a functional leucine-rich NES between residues 240 and 255, in close proximity to or perhaps even overlapping with the region important for nuclear localization. Lastly, this region (residues 240–258), important for both nuclear import and export, is contained in the α-helix as well as two strands of the β-sheets. In particular, the critical residues of the NES are immersed within the hydrophobic β-sandwich structure and are less-than-optimally accessible (Figure 7B; Leu 247 and Ile 249 lie in the midst of strand S2). This raises the possibility that truncation of the CRD (e.g., 136–263, in which all of β-strand S1 in Figure 7B has been deleted, exposing the critical residues of the NES in strand S2) disrupts the β-pleated structure and exposes the NES, which could then override the nuclear localization. To test this hypothesis, we determined the effect of LMB on the localization of GFP–MBP–Gal3(136–263). Indeed, LMB shifted the fluorescence distribution in favor of the nucleus [Figure 4, compare GFP–MBP–Gal3(136–263) with and without

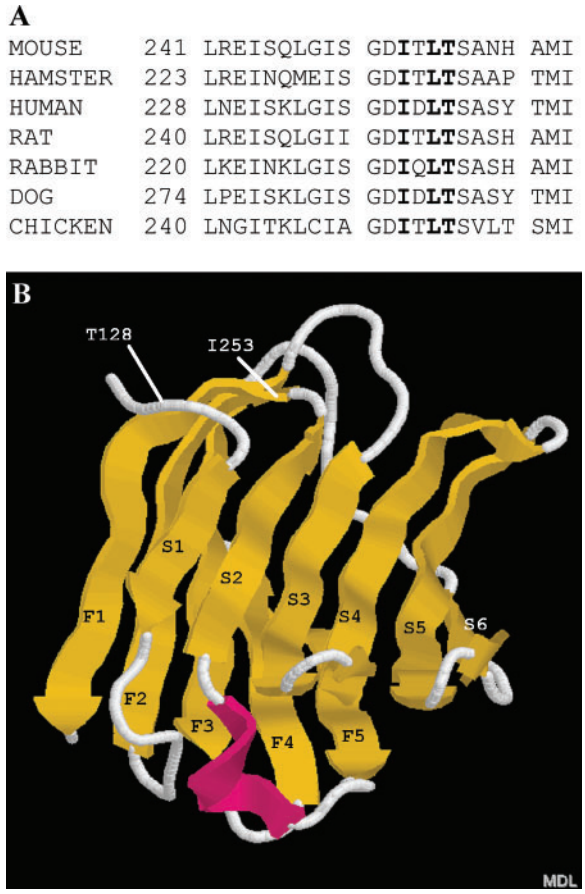

Fig. 7. (**A**) The amino acid sequence of the carboxyl-terminal 23 residues of the Gal3 polypeptide. The murine polypeptide, on which mutagenesis in the present study was carried out, is shown at the top. The sequences of homologs in several other species are also shown for comparison. Residue numbers corresponding to the positions in the polypeptides of the respective species are shown on the left. The conserved I-LT residues shown to be important in nuclear localization are highlighted in boldface type. (**B**) Ribbon diagram showing the three-dimensional structure of the polypeptide backbone of the CRD of Gal3. Residues have been labeled according to the murine polypeptide examined in this study. The thick ribbons highlight the strands of two β-pleated sheets that form the core of the structure. One β-sheet contains five strands (F1–F5); the other β-sheet contains six strands (S1–S6). The white threads connecting the two β-sheets through strands F5 and S2 are bordered by His 236 through Ser 245 and contain the solvent exposed helix (Leu 241 through Ile 244, in fuchsia). The residues determined to be critical for nuclear import begin with I253 at the beginning of strand F1.

LMB; $p < 0.0001$]. These results are consistent with the notions that (a) in the native conformation of the CRD, the nuclear localization activity predominates over a cryptic NES, which may be transiently masked to regulate nuclear localization, and (b) upon disruption of the native structure, the nuclear localization activity residing in the carboxyl-terminal residues of the Gal3 polypeptide is revealed only after inhibition of the NES.

In the same vein, we also tested the effect of LMB on the triple mutant, GFP–MBP–Gal3(1–263; I253A; L255A; T256A). In this case, however, the addition of the drug failed to shift the fluorescence distribution significantly in favor of the nucleus (Figure 6). This would suggest that the observed cytoplasmic localization of the mutant fusion

protein was due to the disruption of nuclear localization activity, rather than to the exposure of the NES.

Discussion

The murine Gal3 polypeptide contains 264 amino acids (Swiss Protein Database, Swiss-Prot # P16110). Measurements of the solution molecular weight of the purified protein by hydrodynamic (Roff and Wang, 1983) or by thermodynamic methods (Morris *et al*., 2004) yielded a value of ~30,000, suggesting that the polypeptide exists predominantly as a monomer. Although this is of a size that could be accommodated by the aqueous channel of the nuclear pore complex (exclusion limit of 40–60 kDa; for reviews, see Nigg, 1997; Gorlich and Kutay, 1999), two lines of evidence argue against the notion that passive diffusion could account for the observed nuclear localization of Gal3.

First, analysis of Gal3 in cell fractions suggests that the protein is associated with high-molecular-weight complexes inside cells: (a) in ~40S particle when nuclear extracts are fractionated on a sucrose gradient (Laing and Wang, 1988) and (b) in a ~670 kDa complex when the transported fraction of a nuclear export assay in permeabilized cells is fractionated by gel filtration (Tsay *et al*., 1999). Second, there are reports in which an exclusively cytoplasmic localization of Gal3 in one cell type can be altered to yield a predominantly nuclear phenotype and vice versa. For example, Gal3 is cytoplasmic in quiescent cultures of 3T3 fibroblasts, but it relocates to the nuclear compartment upon serum stimulation (Moutsatsos *et al*., 1987). In the LG1 strain of human diploid fibroblasts, Gal3 can be found in both the nucleus and the cytoplasm of young, proliferating cells; in contrast, the protein was predominantly cytoplasmic in senescent LG1 cells that have lost replicative competence through in vitro culture (Openo *et al*., 2000). In heterodikaryons derived from fusion of young and senescent LG1 cells, the predominant phenotype was galectin-3 in both nuclei, suggesting that the senescent cells might lack a factor(s) specifically required for Gal3 nuclear import. Conversely, Gal3 has been reported to be concentrated in the nuclei of differentiated colonic epithelial cells. The progression from normal mucosa to adenoma to carcinoma is characterized by a distinct absence of Gal3 in the nuclei of adenoma and carcinoma cells (Lotz *et al*., 1993). Thus, the finding that Gal3 can show a predominantly nuclear localization under one set of conditions and a prominent cytoplasmic localization under other conditions suggests specific and regulated mechanisms of balance between cytoplasmic anchorage, nuclear import, nuclear retention, and nuclear export.

The results of the present study indicate that the carboxyl-terminal region of the murine Gal3 polypeptide is important for nuclear localization, as assayed using a GFP–MBP–Gal3 reporter system. The critical residues include I253, L255, and T256, fitting the IXLT motif identified to be important for the nuclear localization of the *Drosophila* protein Dsh (Itoh *et al*., 2005), in which the IXLT residues also reside in a single strand of a β-sheet (Cheyette *et al*., 2002). These residues are strictly conserved in the amino acid sequences of Gal3 derived from various species (Figure 7A) (Herrmann *et al*., 1993; Mehul *et al*., 1994; Gaudin *et al*., 1995; Nurminskaya and Linsenmayer, 1996). In contrast, the residue corresponding to X in the IXLT motif is not conserved in the same sequences, consistent with our observation that a site-directed mutation at this residue resulted in the least deleterious effect on nuclear localization. Our results need to be compared with those reported by two other laboratories that have attempted to define the region of the Gal3 polypeptide important for nuclear localization.

Gong *et al*. (1999) reported that deletion of the amino-terminal 11 amino acids of human Gal3 resulted in a mutant exhibiting cytoplasmic (and no nuclear) localization in BT-549, a human breast carcinoma cell line. Moreover, when the sequence corresponding to the first 11 amino acids was fused to GFP, a predominantly nuclear distribution of the reporter was observed. On the basis of these and other data, the authors concluded that the 11 residues at the amino terminus are involved in Gal3 translocation to the nucleus (Gong *et al*., 1999). However, the nuclear localization of our mutants truncated from the amino-terminal end [e.g., GFP–MBP–Gal3(121–263)] and the cytoplasmic localization of our mutants truncated from the carboxyl-terminal end [e.g., GFP–MBP–Gal3(1–252)] are clearly inconsistent with the results and conclusion of Gong *et al*. (1999).

In contrast to the results of Gong *et al*. (1999), Gaudin *et al*. (2000) transfected Cos-7 (SV40 virus-transformed monkey kidney) cells and Rb-1 (rabbit smooth muscle) cells with cDNAs encoding mutants of hamster Gal3 containing amino-terminal or internal deletions and showed that nuclear localization does not require the first 103 amino acid residues. Further deletion of residues 104–110 drastically reduced nuclear localization, but the specific sequence between residues 104–110 was not obligatory (these residues could be substituted by an unrelated sequence). These residues correspond to 121–128 in the murine sequence (Mehul *et al*., 1994). Gaudin *et al*. (2000) concluded that nuclear localization of Gal3 does not require determinants in the amino-terminal domain; rather, the carbohydrate-binding carboxyl-terminal domain was sufficient to allow nuclear localization. In this respect, our present results are in good agreement with their results and conclusions. This is particularly significant because the Gaudin *et al*. (2000) study monitored the localization of untagged Gal3 (and fragments) and we monitored the localization of Gal3 (and fragments) in the form of a fusion protein with GFP and MBP. Thus, it is unlikely that there could be sequences important for nuclear localization in the amino-terminal domain that are masked due to the presence of the added fusion proteins.

The three-dimensional structure of the carboxyl-terminal CRD of Gal3 has been determined by X-ray crystallography (Seetharaman *et al*., 1998). Like the CRDs of other members of the galectin family, the Gal3 structure is composed of two β-pleated sheets associated in a sandwich-like arrangement (Figure 7B). One of the β-sheets contains five anti-parallel strands and the other sheet contains six anti-parallel strands. A solvent-exposed α-helix (highlighted in Figure 7B) connects the five-stranded sheet with the six-stranded sheet. Residues 240–258 of the Gal3 sequence,

identified to be important for both nuclear import and export, are found in this region of the three-dimensional structure. In particular, L241 and I244 that start the leucine-rich NES motif are found in the helix, but L247 and I249, critical for NES activity (Li *et al.*, 2006), are found sequestered in the adjacent β-sheet. In the native conformation, the signal for nuclear export appears to be cryptic (or at least subservient to the signal for nuclear import). Disruption of the six-stranded β-sheet by deletion mutagenesis appears to unravel the β-sandwich, exposing L247 and I249 that are required for NES activity.

This notion is supported by several observations made by Gaudin *et al.* (2000) and by ourselves in the present study. First, deletion from the amino terminus up to G103 in the hamster sequence and G121 of the mouse sequence results in nuclear localization, like the full-length Gal3 polypeptide. When the sequences of the two species are aligned, hamster G103 corresponds exactly to murine G121 (Mehul *et al.*, 1994). Similarly, T110 of the hamster sequence corresponds exactly to murine T128, in which we observed a shift in the histogram distribution with loss of nuclear localization in favor of the cytoplasm. In the three-dimensional structure, this is just before the first strand in the six-stranded β-sheet (Figure 7B). Second, the effect of NES exposure can be counterbalanced through inhibition of the CRM1 exportin by LMB. Thus, the cytoplasmic localization of GFP–MBP–Gal3(136–263) is shifted to more nuclear localization in the presence of LMB (Figure 4). Third, the association of the two β-sheets in the sandwich-like structure appears to be important for the native conformation of the CRD, as revealed by carbohydrate-binding activity. In studying bovine Gal1, which consists of a single domain (the CRD), Abbott and Feizi (1991) noted that almost the entire polypeptide is necessary for integrity of lactose binding. Deletion of the first nine residues from the amino terminus resulted in loss of ~70% of the activity. When the sequences of the CRDs are aligned (Hirabayashi, 1997), this would correspond to truncation at residue 137 of the murine Gal3 polypeptide. The observation of Gaudin *et al.* (2000) that the specific sequence between residues 104 and 110 of hamster Gal3 was not necessary for nuclear localization but could be substituted by an unrelated sequence is rationalized in terms of preserving the β-sandwich structure.

It is also important to point out, however, that the effect of the point mutations on Gal3 localization cannot be explained simply by an unraveling of the β-sandwich. We have surveyed alanine mutations at dozens of other residues within the CRD with the following sample of qualitative results: (a) most have little effect on the localization of Gal3 fusion proteins, as illustrated by L147 and M238 (hydrophobic residues found in strands S3 and F5 in Figure 7B, respectively), R157, which is involved in carbohydrate recognition (Seetharaman *et al.*, 1998), and N240, a hydrophilic residue in strand S2; (b) a few others do have effect, as shown by L247 (more nuclear, as reported in Li *et al.*, 2006) and I249 (less nuclear, as reported in Li *et al.*, 2006). In further support of this notion, double and quadruple point mutants in Gal1 in the region corresponding to residues 252–263 of murine Gal3 had little effect on carbohydrate binding (Abbott and Feizi, 1991).

It should be emphasized that we do not know whether the region of Gal3 important for nuclear localization (residues 252–258) represents a binding site for a nuclear import receptor (importin-β or a relative). Alternatively, this sequence could simply represent a binding site for another nuclear protein that carries a bona fide NLS mediated by a well-characterized importin. Several interacting partners of Gal3 have been identified in the nucleus: (a) Gemin4 (Park *et al.*, 2001), (b) thyroid-specific transcription factor (Paron *et al.*, 2003), (c) CBP70 (Seve *et al.*, 1993), (d) Sufu (suppressor of fused in the Hedgehog signaling pathway) (Paces-Fessy *et al.*, 2004), and (e) β-catenin (Shimura *et al.*, 2004). However, the mechanism(s) and signal(s) responsible for their nuclear localization, alone or in complex with Gal3, remain to be elucidated.

Materials and Methods

Preparation of the pEGFP-c_1 vector for expression of the fusion protein GFP–MBP–Gal3

In this study, the analysis of nuclear versus cytoplasmic localization was carried out using a fusion protein (pGMG3) containing Gal3, GFP, and bacterial MBP. In stage 1, the cDNA for Gal3 was liberated from plasmid pWJ31 (Agrwal *et al.*, 1989) by EcoRI digestion and then inserted into the corresponding restriction site of the bacterial expression vector pMAL-c_2x (New England Biolabs, Beverly, MA). Because the plasmid pWJ31 had been constructed from an EcoRI fragment from a λgt11 library, it did not code for the first amino acid in Gal3; therefore, full-length Gal3 in the study consisted of 263 amino acids, rather than the 264 of native murine Gal3. In stage II, this plasmid encoding the fusion protein MBP–Gal3 was used as the template for polymerase chain reaction (PCR) amplification, using the following primers: 5′-GGG GGT ACC ATG AAA ATC GAA GAA GGT AAA C-3′ (which generates the KpnI restriction site not on the template); 5′-AGG TCG ACT CTA GAG GAT C-3′ (which reproduces the BamHI site on the template). In stage III, this PCR product was ligated into the mammalian expression vector, pEGFP-c_1 (Clontech, San Jose, CA). The expression of the fusion protein GFP–MBP–Gal3 from pGMG3 in transfected cells is driven by a cytomegalovirus promoter. The vector for the production of GFP-Gal3 was prepared from the respective cDNAs in a similar fashion.

Mutants in which the Gal3 sequence was truncated from the carboxyl terminus were generated by introducing stop codons at specific positions in the pGMG3 plasmid. Using the QuikChange Site-Directed Mutagenesis Kit (Strategene, La Jolla, CA), this was carried out at amino acid residues 262, 261, 260, 259, 258, 253, and 232. For example, insertion of a stop codon at position 259 resulted in the fusion protein GFP–MBP–Gal3(1–258).

The pGMG3 plasmid contains three EcoRI restriction sites: (a) between GFP and MBP, (b) at the 5′ end of the Gal3 coding sequence, and (c) at the 3′ end of the Gal3 sequence. Site-directed mutagenesis (5′-CAT CCC GGA CTT CGG ATC CAC C-3′ and 5′-G GTG GAT CCG AAG TCC GGG ATG-3′) was carried out to remove the last of these EcoRI sites. The resulting plasmid was used as

the template to remove the first EcoRI site, between the GFP and MBP sequences (5′-CGA GCT CAA GCT TCG ACT TCT GCA GTC GAC GG-3′ and 5′-CC GTC GAC TGC AGA AGT CGA AGC TTG AGC TCG-3′). This provided the starting material for the generation of mutants in which the Gal3 sequence was truncated from the amino terminus. Site-directed mutagenesis was carried out to insert EcoRI sites into specific positions of the Gal3 sequence. After digestion with the restriction enzyme, the isolated DNA was religated with T4 DNA ligase. The following forward and reverse primers were used to obtain the respective GFP–MBP–Gal3 mutants: (a) for (74–263), 5′-CCT AGT GCC TAC CCC GAA TTC ACT ACT GCC CCT GGA GC-3′ and 5′-GC TCC AGG GGC AGT GAA TTC GGG GTA GGC ACT AGG-3′; (b) for (121–263), 5′-GC TAT CCT GCT GCT GGC GAA TTC GGT GTC CCC GCT GGA CC-3′ and 5′-GG TCC AGC GGG GAC ACC GAA TTC GCC CGA AGC AGG ATA GC-3′; (c) for (128–263), 5′-GGT GTC CCC GCT GGA GAA TTC ACG GTG CCC TAT GAC-3′ and 5′-GTC ATA GGG CAC CGT GAA TTC TCC AGC GGG GAC ACC-3′; (d) for (131–263), 5′-GGT GTC CCC GCT GGA GAA TTC ACG GTG CCC TAT GAC-3′ and 5′-GTC ATA GGG CAC CGT GAA TTC TCC AGC GGG GAC ACC-3′; (e) for (136–263), 5′-GTG CCC TAT GAC CTG GAA TTC CCT GGA GGA GTC ATG C-3′ and 5′-G CAT GAC TCC TCC AGG GAA TTC CAG GTC ATA GGG CAC-3′; (f) for (I253A), 5′-GGG ATC AGT GGT GAC GCA ACC CTC ACC AGC GC-3′ and 5′-GCG CTG GTG AGG GTT GCG TCA CCA CTG ATC CC-3′; (g) for (T254A), 5′-GAT CAG TGG TGA CAT AGC CCT CAC CAG CGC TAA C-3′ and 5′-GTT AGC GCT GGT GAG GGC TAT GTC ACC ACT GAT C-3′; (h) for (L255A), 5′-CAG TGG TGA CAT AAC CGC CAC CAG CGC TAA CCA C-3′ and 5′-CTG GTT AGC GCT GGT GGC GGT TAT GTC ACC ACT G-3′; (i) for (T256A), 5′-GGT GAC ATA ACC CTC GCC AGC GCT AAC CAC G-3′ and 5′-CGT GGT TAG CGC TGG CGA GGG TTA TGT CAC C-3′; and (j) for (I253A; L255A; T256A), 5′-GGT GAC GCA ACC GCC GCC AGC GCT AAC CAC G-3′ and 5′-C GTG GTT AGC GCT GGC GGC GGT TGC GTC ACC-3′.

Cell culture and transfection

NIH mouse 3T3 fibroblasts were obtained from the American Type Culture Collection (Rockville, MD). The cells were grown as monolayers in Dulbecco's modified Eagle's medium (DMEM) containing 10% calf serum, 100 U/ml of penicillin, and 100 μg/ml of streptomycin at 37°C in a humidified atmosphere of 10% CO_2 (Steck *et al.*, 1979). Cells were transfected with vectors expressing fusion proteins containing the GFP reporter group described above. For transfections to be analyzed by immunoblotting, the cells were cultured and transfected in 60-mm plates (29 cm^2 growth surface). For transfections to be analyzed by fluorescence, the cells were cultured on glass coverslips in 35-mm plates (10 cm^2 growth surface). The following describes the protocol used for transfection of a single 35-mm plate; for transfection of 60-mm plates, the amounts of reagents used are increased 3-fold correspondingly.

Cells were seeded at a density of 1×10^4 cells/cm^2 and cultured overnight. A 100 μl solution of serum-free DMEM containing 1 μg of the DNA construct was mixed with 100 μl of serum-free DMEM containing 3 μl of lipofectamine (Invitrogen, Carlsbad, CA; 2 mg/ml). The cells in the culture plate were washed with serum-free DMEM and the 200 μl mixture containing DNA and lipofectamine was added, along with 0.8 ml of serum-free DMEM. The plate was placed in the CO_2 incubator for 3 h, at which time 1 ml of DMEM containing 20% calf serum was added. The plate was incubated for another 6 h. The medium in the plate was then replaced with 2 ml of fresh DMEM containing 10% calf serum. In some experiments, CHX (Boehringer Mannheim, Indianapolis, IN; 10 μg/ml final concentration) and LMB (LC Laboratories, Woburn, MA; 5.4 ng/ml [10 nM] final concentration) were included during this medium change. The cells were incubated for an additional 5 h, at which time they were processed for fluorescence analysis (see *Fluorescence microscopy*). For immunoblotting analysis, the cells in 60-mm plates were incubated for 24 h after the medium change before harvesting for preparation of lysates.

Fluorescence microscopy

For the examination of the transfected cells by fluorescence microscopy, the coverslips were first washed three times with ice-cold phosphate-buffered saline (PBS). The cells were then fixed by treating for 20 min in 2 ml of 4% paraformaldehyde in PBS at room temperature. The cells were washed twice (10 min each, 3 ml PBS) at room temperature. Finally, the coverslips were mounted on glass microscope slides using Perma-Fluor (Thermo Shandon, Pittsburgh, PA). In some experiments, we had also transfected cells cultured in Lab-Tek Chamber slides (Nalge Nunc International, Naperville, IL) using the same conditions as described for the transfection of the cells cultured on coverslips in 35-mm plates. The results obtained with GFP fluorescence in the live cells in chamber slides and fixed cells on coverslips were essentially the same.

We also compared the localization of the GFP-MalE-Gal3 reporter against the localization of endogenous Gal3 in the 3T3 fibroblasts. Endogenous Gal3 was detected using the rat monoclonal antibody, anti-Mac2 (25 μg/ml in PBS containing 0.2% gelatin) and fluorescein-conjugated goat anti-rat immunoglobulin (Sigma, St. Louis, MO; 1:500 dilution). The details of the indirect immunofluorescence protocol have been previously described (Tsay *et al.*, 1999).

Fluorescent cells were examined using a Meridian Instruments (Okemos, MI) Insight confocal laser-scanning microscope. For each construct, we scored the fluorescence labeling pattern in each cell into one of five categories: (a) exclusively nuclear (N), (b) intensely nuclear over a cytoplasmic background (N > C), (c) equal distribution between the nucleus and cytoplasm (N ~ C), (d) less nuclear labeling than in the cytoplasm (N < C), and (e) exclusively cytoplasmic (C). Data were collected from three independent experiments in which at least 100 fluorescent cells were scored for the localization of GFP fluorescence. The mean number of cells scored to each localization was plotted in

the form of histograms with standard error of the mean. Representative cells were photographed at low magnification to show a field containing multiple cells and at high magnification to show a single cell.

The number of cells scored into each category of localization was tabulated from triplicate experiments. Chi-square analyses were carried out using the statistical analysis program StatView, version 5.0.1 (SAS Institute, Cary, NC). The analyses were performed using the "Contingency Table" function, selecting "Coded summary data" and deselecting "Fisher's Exact Test."

SDS–PAGE and immunoblotting

Proteins were resolved on SDS–PAGE (10% acrylamide) as described by Laemmli (1970). The procedures for immunoblotting after SDS–PAGE have also been described (Tsay *et al*., 1999). The antibodies used for immunoblotting and their sources were (a) polyclonal anti-GFP (Clontech), (b) anti-MBP (New England Biolabs), and (c) polyclonal anti-Gal3 (#32 and #33, see Agrwal *et al*., 1993).

Three-dimensional visualization of Gal3

Images of the CRD of Gal3 (Research Collaboratory for Structural Bioinformatics Protein Databank, PDB # 1KJL) bound to *N*-acetyl lactosamine were generated using Protein Explorer found at http://proteinexplorer.org (Martz, 2002).

Acknowledgments

We thank Richard Gray, Jennifer Bender, and Dan Neef for their help in the construction of the vector for expressing the fusion protein, GFP–MBP–Gal3, during the early part of the study. EJA thanks Lori Keen and Stephen Matheson for their assistance with the cell culture facilities at Calvin College. This work was supported by a 2003 Merck/AAAS Undergraduate Science Research Program Grant (to EJA), a Calvin Research Fellowship from Calvin College (to EJA), and by grants Cottrell College Science Award from the Research Corporation (to EJA), GM-38740 from the National Institutes of Health (to JLW), and MCB-0092919 from the National Science Foundation (to RJP).

Conflict of interest statement

None declared.

Abbreviations

CHX, cycloheximide; CRD, carbohydrate-recognition domain; DMEM, Dulbecco's modified Eagle's medium; Gal1, galectin-1; Gal3, galectin-3; GFP, green fluorescent protein; LMB, leptomycin B; MBP or MalE, maltose-binding protein; NES, nuclear export signal; PBS, phosphate-buffered saline; PCR, polymerase chain reaction; RNP, ribonucleoprotein complex; SMN, survival of motor neuron protein.

References

Abbott, W.M. and Feizi, T. (1991) Soluble 14-kDa beta-galactoside-specific bovine lectin. Evidence from mutagenesis and proteolysis that almost the complete polypeptide chain is necessary for integrity of the carbohydrate recognition domain. *J. Biol. Chem.*, **266**, 5552–5557.

Agrwal, N., Sun, Q., Wang, S.Y., and Wang, J.L. (1993) Carbohydrate-binding protein 35. I. Properties of the recombinant polypeptide and the individuality of the domains. *J. Biol. Chem.*, **268**, 14932–14939.

Agrwal, N., Wang, J.L., and Voss, P.G. (1989) Carbohydrate-binding protein 35. Levels of transcription and mRNA accumulation in quiescent and proliferating cells. *J. Biol. Chem.*, **264**, 17236–17242.

Alefantis, T., Barmak, K., Harhaj, E.W., Grant, C., and Wigdahl, B. (2003) Characterization of a nuclear export signal within the human T cell leukemia virus type I transactivator protein Tax. *J. Biol. Chem.*, **278**, 21814–21822.

Barondes, S.H., Castronovo, V., Cooper, D.N., Cummings, R.D., Drickamer, K., Feizi, T., Gitt, M.A., Hirabayashi, J., Hughes, C., Kasai, K., et al. (1994) Galectins: a family of animal beta-galactoside-binding lectins. *Cell*, **76**, 597–598.

Cheyette, B.N., Waxman, J.S., Miller, J.R., Takemaru, K., Sheldahl, L.C., Khlebtsova, N., Fox, E.P., Earnest, T., and Moon, R.T. (2002) Dapper, a dishevelled-associated antagonist of beta-catenin and JNK signaling, is required for notochord formation. *Dev. Cell*, **2**, 449–461.

Dagher, S.F., Wang, J.L., and Patterson, R.J. (1995) Identification of galectin-3 as a factor in pre-mRNA splicing. *Proc. Natl Acad. Sci. U. S. A.*, **92**, 1213–1217.

Davidson, P.J., Davis, M.J., Patterson, R.J., Ripoche, M.A., Poirier, F., and Wang, J.L. (2002) Shuttling of galectin-3 between the nucleus and cytoplasm. *Glycobiology*, **12**, 329–337.

Fischer, U., Liu, Q., and Dreyfuss, G. (1997) The SMN–SIP1 complex has an essential role in spliceosomal snRNP biogenesis. *Cell*, **90**, 1023–1029.

Gaudin, J.C., Mehul, B., and Hughes, R.C. (2000) Nuclear localisation of wild type and mutant galectin-3 in transfected cells. *Biol. Cell*, **92**, 49–58.

Gaudin, J.C., Monsigny, M., and Legrand, A. (1995) Cloning of the cDNA encoding rabbit galectin-3. *Gene*, **163**, 249–252.

Gong, H.C., Honjo, Y., Nangia-Makker, P., Hogan, V., Mazurak, N., Bresalier, R.S., and Raz, A. (1999) The NH_2 terminus of galectin-3 governs cellular compartmentalization and functions in cancer cells. *Cancer Res.*, **59**, 6239–6245.

Gorlich, D. and Kutay, U. (1999) Transport between the cell nucleus and the cytoplasm. *Annu. Rev. Cell Dev. Biol.*, **15**, 607–660.

Herrmann, J., Turck, C.W., Atchison, R.E., Huflejt, M.E., Poulter, L., Gitt, M.A., Burlingame, A.L., Barondes, S.H., and Leffler, H. (1993) Primary structure of the soluble lactose binding lectin L-29 from rat and dog and interaction of its non-collagenous proline-, glycine-, tyrosine-rich sequence with bacterial and tissue collagenase. *J. Biol. Chem.*, **268**, 26704–26711.

Hirabayashi, J. (1997) Recent topics on galectins. *Trends Glycosci. Glycotechnol.*, **84**, 1–184.

Hubert, M., Wang, S.Y., Wang, J.L., Seve, A.P., and Hubert, J. (1995) Intranuclear distribution of galectin-3 in mouse 3T3 fibroblasts: comparative analyses by immunofluorescence and immunoelectron microscopy. *Exp. Cell Res.*, **220**, 397–406.

Itoh, K., Brott, B.K., Bae, G.U., Ratcliffe, M.J., and Sokol, S.Y. (2005) Nuclear localization is required for dishevelled function in Wnt/beta-catenin signaling. *J. Biol.*, **4**, 3.

Laemmli, U.K. (1970) Cleavage of structural proteins during the assembly of the head of bacteriophage T4. *Nature*, **227**, 680–685.

Laing, J.G. and Wang, J.L. (1988) Identification of carbohydrate binding protein 35 in heterogeneous nuclear ribonucleoprotein complex. *Biochemistry*, **27**, 5329–5334.

Li, S.Y., Davidson, P.J., Lin, N.Y., Patterson, R.J., Wang, J.L., and Arnoys, E.J. (2006) Transport of galectin-3 between the nucleus and cytoplasm. II. Identification of the signal for nuclear export, *Glycobiology*, **16**.

Liu, F.T., Patterson, R.J., and Wang, J.L. (2002) Intracellular functions of galectins. *Biochim. Biophys. Acta*, **1572**, 263–273.

Liu, Q. and Dreyfuss, G. (1996) A novel nuclear structure containing the survival of motor neurons protein. *EMBO J.*, **15**, 3555–3565.

Lotz, M.M., Andrews, C.W., Jr, Korzelius, C.A., Lee, E.C., Steele, G.D., Jr, Clarke, A., and Mercurio, A.M. (1993) Decreased expression of Mac-2 (carbohydrate binding protein 35) and loss of its nuclear localization are

associated with the neoplastic progression of colon carcinoma. *Proc. Natl Acad. Sci. U. S. A.*, **90**, 3466–3470.

Martz, E. (2002) Protein explorer: easy yet powerful macromolecular visualization. *Trends Biochem. Sci.*, **27**, 107–109.

Mehul, B., Bawumia, S., Martin, S.R., and Hughes, R.C. (1994) Structure of baby hamster kidney carbohydrate-binding protein CBP30, an S-type animal lectin. *J. Biol. Chem.*, **269**, 18250–18258.

Meister, G., Eggert, C., and Fischer, U. (2002) SMN-mediated assembly of RNPs: a complex story. *Trends Cell Biol.*, **12**, 472–478.

Morris, S., Ahmad, N., Andre, S., Kaltner, H., Gabius, H.J., Brenowitz, M., and Brewer, F. (2004) Quaternary solution structures of galectins-1, -3, and -7. *Glycobiology*, **14**, 293–300.

Moutsatsos, I.K., Wade, M., Schindler, M., and Wang, J.L. (1987) Endogenous lectins from cultured cells: nuclear localization of carbohydrate-binding protein 35 in proliferating 3T3 fibroblasts. *Proc. Natl. Acad. Sci. U. S. A.*, **84**, 6452–6456.

Nigg, E.A. (1997) Nucleocytoplasmic transport: signals, mechanisms and regulation. *Nature*, **386**, 779–787.

Nurminskaya, M. and Linsenmayer, T.F. (1996) Identification and characterization of up-regulated genes during chondrocyte hypertrophy. *Dev. Dyn.*, **206**, 260–271.

Openo, K.P., Kadrofske, M.M., Patterson, R.J., and Wang, J.L. (2000) Galectin-3 expression and subcellular localization in senescent human fibroblasts. *Exp. Cell Res.*, **255**, 278–290.

Ossareh-Nazari, B., Bachelerie, F., and Dargemont, C. (1997) Evidence for a role of CRM1 in signal-mediated nuclear protein export. *Science*, **278**, 141–144.

Paces-Fessy, M., Boucher, D., Petit, E., Paute-Briand, S., and Blanchet-Tournier, M.F. (2004) The negative regulator of Gli, Suppressor of fused (Sufu), interacts with SAP18, galectin3 and other nuclear proteins. *Biochem. J.*, **378**, 353–362.

Park, J.W., Voss, P.G., Grabski, S., Wang, J.L., and Patterson, R.J. (2001) Association of galectin-1 and galectin-3 with Gemin4 in complexes containing the SMN protein. *Nucleic Acids Res.*, **29**, 3595–3602.

Paron, I., Scaloni, A., Pines, A., Bachi, A., Liu, F.T., Puppin, C., Pandolfi, M., Ledda, L., Di Loreto, C., Damante, G., and Tell, G. (2003) Nuclear localization of galectin-3 in transformed thyroid cells: a role in transcriptional regulation. *Biochem. Biophys. Res. Commun.*, **302**, 545–553.

Pellizzoni, L., Kataoka, N., Charroux, B., and Dreyfuss, G. (1998) A novel function for SMN, the spinal muscular atrophy disease gene product, in pre-mRNA splicing. *Cell*, **95**, 615–624.

Roff, C.F. and Wang, J.L. (1983) Endogenous lectins from cultured cells. Isolation and characterization of carbohydrate-binding proteins from 3T3 fibroblasts. *J. Biol. Chem.*, **258**, 10657–10663.

Seetharaman, J., Kanigsberg, A., Slaaby, R., Leffler, H., Barondes, S.H., and Rini, J.M. (1998) X-ray crystal structure of the human galectin-3 carbohydrate recognition domain at 2.1-A resolution. *J. Biol. Chem.*, **273**, 13047–13052.

Seve, A.P., Felin, M., Doyennette-Moyne, M.A., Sahraoui, T., Aubery, M., and Hubert, J. (1993) Evidence for a lactose-mediated association between two nuclear carbohydrate-binding proteins. *Glycobiology*, **3**, 23–30.

Sherman, M.P., de Noronha, C.M., Heusch, M.I., Greene, S., and Greene, W.C. (2001) Nucleocytoplasmic shuttling by human immunodeficiency virus type 1 Vpr. *J. Virol.*, **75**, 1522–1532.

Shimura, T., Takenaka, Y., Tsutsumi, S., Hogan, V., Kikuchi, A., and Raz, A. (2004) Galectin-3, a novel binding partner of beta-catenin. *Cancer Res.*, **64**, 6363–6367.

Steck, P.A., Voss, P.G., and Wang, J.L. (1979) Growth control in cultured 3T3 fibroblasts. Assays of cell proliferation and demonstration of a growth inhibitory activity. *J. Cell Biol.*, **83**, 562–575.

Tsay, Y.G., Lin, N.Y., Voss, P.G., Patterson, R.J., and Wang, J.L. (1999) Export of galectin-3 from nuclei of digitonin-permeabilized mouse 3T3 fibroblasts. *Exp. Cell Res.*, **252**, 250–261.

Vyakarnam, A., Dagher, S.F., Wang, J.L., and Patterson, R.J. (1997) Evidence for a role for galectin-1 in pre-mRNA splicing. *Mol. Cell Biol.*, **17**, 4730–4737.